Development 134, 2159-2169 (2007) doi:10.1242/dev.001586

Conditional *Kif3a* ablation causes abnormal hedgehog signaling topography, growth plate dysfunction, and excessive bone and cartilage formation during mouse skeletogenesis

Eiki Koyama[1,‡], Blanche Young[1], Motohiko Nagayama[1], Yoshihiro Shibukawa[1,*], Motomi Enomoto-Iwamoto[1], Masahiro Iwamoto[1], Yukiko Maeda[2], Beate Lanske[2], Buer Song[3,†], Rosa Serra[3] and Maurizio Pacifici[1,‡]

The motor protein Kif3a and primary cilia regulate important developmental processes, but their roles in skeletogenesis remain ill-defined. Here we created mice deficient in *Kif3a* in cartilage and focused on the cranial base and synchondroses. *Kif3a* deficiency caused cranial base growth retardation and dysmorphogenesis, which were evident in neonatal animals by anatomical and micro-computed tomography (μCT) inspection. *Kif3a* deficiency also changed synchondrosis growth plate organization and function, and the severity of these changes increased over time. By postnatal day (P)7, mutant growth plates lacked typical zones of chondrocyte proliferation and hypertrophy, and were instead composed of chondrocytes with an unusual phenotype characterized by strong collagen II (*Col2a1*) gene expression but barely detectable expression of Indian hedgehog (*Ihh*), collagen X (*Col10a1*), *Vegf* (*Vegfa*), *MMP-13* (*Mmp13*) and osterix (*Sp7*). Concurrently, unexpected developmental events occurred in perichondrial tissues, including excessive intramembranous ossification all along the perichondrial border and the formation of ectopic cartilage masses. Looking for possible culprits for these latter processes, we analyzed hedgehog signalling topography and intensity by monitoring the expression of the hedgehog effectors Patched 1 and Gli1, and of the hedgehog-binding cell-surface component syndecan 3. Compared with controls, hedgehog signaling was quite feeble within mutant growth plates as early as P0, but was actually higher and was widespread all along mutant perichondrial tissues. Lastly, we studied postnatal mice deficient in *Ihh* in cartilage; their cranial base defects only minimally resembled those in *Kif3a*-deficient mice. In summary, Kif3a and primary cilia make unique contributions to cranial base development and synchondrosis growth plate function. Their deficiency causes abnormal topography of hedgehog signaling, growth plate dysfunction, and un-physiologic responses and processes in perichondrial tissues, including ectopic cartilage formation and excessive intramembranous ossification.

KEY WORDS: Kif3a, Primary cilia, Cranial base synchondroses, Hedgehog signaling, Syndecans, Growth plate, Intramembranous ossification, Ectopic cartilage, Exostoses, Mouse

INTRODUCTION

Kif3a is an essential component of the intraflagellar transport (IFT) motor system of primary cilia (Rosenbaum and Witman, 2002). These organelles, which were first described decades ago, are microtubule-containing non-motile structures protruding from the surface of most vertebrate cells (Scherft and Daems, 1967; Sorokin, 1968). Recent studies have shown that primary cilia are important regulators of cell and tissue function, and of developmental processes. Mutations in the structural and functional components of primary cilia can cause serious human conditions, including polycystic kidney disease and retinal degeneration (Ansley et al., 2003; Lin et al., 2003; Pazour et al., 2000). Similarly, altered primary cilia function can have damaging repercussions on limb patterning, neural tube formation and other major developmental processes (Huangfu et al., 2003; Murcia et al., 2000; Zhang et al., 2003). The importance and centrality of primary cilia in both health and disease reflect the fact that these organelles and their IFT system have turned out to mediate and transduce intercellular chemical, physical and biological signals (Davenport and Yoder, 2005), including those elicited by hedgehog proteins (Corbit et al., 2005; Haycraft et al., 2005; May et al., 2005). These proteins are well-known regulators of multiple developmental processes (Bitgood and McMahon, 1995; McMahon et al., 2003). They are lipid-containing factors, secreted by donor cells, that diffuse through their surroundings and exert action on short- and long-range target cells (Gritli-Linde et al., 2001; Yin et al., 2002). The proteins act by binding to the cell surface receptor Patched 1 (Ptch1), and signals are transmitted by the receptor smoothened via the zinc-finger transcription factors Gli1, Gli2 and Gli3. Current thinking, which has been reviewed recently (Huangfu and Anderson, 2006; Singla and Reiter, 2006), is that, following hedgehog interaction with Patched 1, smoothened is activated and translocated to the primary cilia via the IFT system, resulting in the production of Gli activator forms that would translocate to the nucleus and activate hedgehog gene target expression. In the absence of hedgehog proteins, smoothened would remain sequestered and inactive, and Gli proteins would be processed into repressor forms and move to the nucleus to inhibit hedgehog target gene expression.

A well-documented target of hedgehog signaling is the developing axial and limb skeleton (Bitgood and McMahon, 1995; Koyama et al., 1996; Lanske et al., 1996). As a recent study from our groups shows, hedgehog signaling is also very important for the

[1]Department of Orthopaedic Surgery, Thomas Jefferson University College of Medicine, Philadelphia, PA 19107, USA. [2]Department of Developmental Biology, Harvard School of Dental Medicine, Boston, MA 02138, USA. [3]Department of Cell Biology, University of Alabama at Birmingham, Birmingham, AL 35294, USA.

*Present address: Department of Periodontology, Tokyo Dental College, Chiba, Japan
†Present address: Department of Orthopaedic Surgery, University of California, Los Angeles, CA, USA
‡Authors for correspondence (e-mails: eiki.koyama@jefferson.edu; maurizio.pacifici@jefferson.edu)

Accepted 30 March 2007

early formation, growth and function of the cranial base and its synchondroses (Young et al., 2006). The synchondroses are cartilaginous palindromic structures each consisting of two mirror-image growth plates and termed ethmoidal, intrasphenoidal, spheno-occipital or intraoccipital according to their anatomical location. They are important for cranial base development and overall growth patterns (Ingervall and Thilander, 1972; Roberts and Blackwood, 1983), and defects in synchondrosis functioning are likely to contribute to craniofacial deformities such as those seen in Crouzon and Apert syndromes (Chen et al., 1999; Kreiborg et al., 1993). We found that synchondrosis development is severely affected in mice lacking the Indian hedgehog (*Ihh*) gene. $Ihh^{-/-}$ cartilaginous cranial bases were short and deficient in extracellular proteoglycan matrix. The mutant synchondroses displayed abnormal chondrocyte proliferation, hypertrophy and topographical arrangement with respect to the perichondrium; as a consequence, endochondral ossification was deranged. In several but not all respects, these abnormalities are reminiscent of those seen in developing $Ihh^{-/-}$ long bones (St-Jacques et al., 1999), pointing to the pivotal nature and general requirement of hedgehog action in skeletogenesis. Given their roles in hedgehog signaling, primary cilia should be as essential for skeletal development and growth as hedgehog proteins, and previous genetic studies certainly support that premise (Murcia et al., 2000; Olsen et al., 2005; Xiao et al., 2006; Zhang et al., 2003). In particular, limb and cranial skeletal abnormalities were found in conditional mouse mutants deficient in *Kif3a* or in the cilia-associated mechanosensory protein polycystin-1 (Pkd1), as well as in mice bearing a missense mutation in the *Pkd1* gene (Olsen et al., 2005; Xiao et al., 2006). A more extensive recent study indicated that long bone anlagen in mouse embryo limbs deficient in *Ift88* or *Kif3a* (*prx1cre;*$Ift88^{fl/n}$ or *prx1cre;*$Kif3a^{fl/n}$) are short, exhibit accelerated chondrocyte hypertrophy and lack an intramembranous bone collar (Haycraft et al., 2007). In the present study, we analyzed mice deficient in *Kif3a* in cartilage and found that cranial base development and growth were also impaired, particularly at postnatal stages. However, mutant synchondroses displayed a delay in chondrocyte hypertrophy, excessive intramembranous ossification along their perichondrial border and ectopic cartilage masses. These defects were associated with a topographical re-distribution of hedgehog signaling that was quite feeble within the mutant growth plates themselves, but was prominent and widespread all along the perichondrial border, thus most likely responsible for the excessive ossification and ectopic cartilage formation. When we examined mice deficient in *Ihh* in cartilage at similar postnatal stages, their synchondrosis defects minimally resembled those of *Kif3a*-deficient mice, pointing to unique contributions and regulatory roles of primary cilia in synchondrosis development and function.

MATERIALS AND METHODS

Conditional *Kif3a* and *Ihh* ablation

Animals used in this study were maintained in accordance with the National Institutes of Health (NIH) Guide for the Care and Use of Laboratory Animals, and protocols were reviewed and approved by the Institutional Animal Care and Use Committee (IACUC) at each of our respective institutions. Homozygous mice deficient in *Kif3a* in cartilage were produced by sequential mating of $Kif3a^{fl/fl}$ mice (Marszalek et al., 1999) with *Col2a1-Cre* transgenic mice (Ovdhinnikov et al., 2000). The genotype of transgenic mice was determined by PCR analyses of genomic DNA isolated from tail or liver. The *Col2a1-Cre* mice were identified by using Primer1: 5′-TGCTCTGTCCGTTTGCCG-3′ and Primer2: 5′-ACTGTGTCCAGACCAGGC-3′, generating one band of approximately 720 bp. The loxP alleles or *Kif3a* were identified using three primers: Primer1: 5′-TCTGTGAGTTTGTGACCAGCC-3′; Primer2: 5′-AGGGCAGACGGAAGGGTGG-3′; and Primer3: 5′-TGGCAGGTCAATGGACGCAG-3′. Homozygous *Kif3a*-deficient mice were born with Mendelian frequency and were studied at postnatal days (P)0, P7 and P15.

Homozygous mice deficient in *Ihh* in postnatal cartilage were produced by sequentially mating $Ihh^{fl/fl}$ mice (Maeda et al., 2007) with *Col2a1-CreER* transgenic mice (Nakamura et al., 2006). The genotyping of mice was performed by PCR using the following specific primers: *fl-Ihh* forward: 5′-AGCACCTTTTTTCTCGACTGCCTG-3′; *fl-Ihh* reverse: 5′-TGTTAGGCCGAGAGGGATTTCGTG-3′; *Cre 275*: 5′-CGCGGTCTGGCAGTAAAAACTATC-3′; *Cre 603*: 5′-CCCACCGTCAGTACGTGAGATATC-3′. After an initial denaturation for 8 minutes at 94°C, amplification cycles consisted of denaturation at 94°C for 30 seconds, annealing at 68°C for 30 seconds and 45 seconds extension at 72°C for 35 cycles, followed by a final extension for 10 minutes at 72°C. The expected amplicons for the wild-type *Ihh* allele were 320 bp, 400 bp for the floxed *Ihh* allele and 328 bp for the *Cre* allele. To verify *Cre* activity and specificity postnatally, *Col2a1-CreER* mice were mated with Rosa R26R reporter mice and resulting double-transgenic mice were injected with 4-hydroxy-tamoxifen (Sigma) at P0 and evaluated for *lacZ* activity at P1, P4, P7 and P14 by histochemistry (Nakamura et al., 2006; Maeda et al., 2007).

Micro-computed tomography, histology and immunohistochemistry

Skulls were fixed in buffered 4% paraformaldehyde overnight at 4°C, rinsed and subjected to micro-computed tomography (μCT) using a μCT40 SCANCO Medical system. Samples were scanned using a 36 mm holder at 45 kV of energy, 12 μm scanning thickness and medium resolution. Two-dimensional slice images were selected and used to generate three-dimensional reconstructions with the following parameters: filter width sigma=0.8, support level=1.0 and threshold=173. The same values were used to analyze wild-type and mutant samples at each specified time point. Three-dimensional images were rotated at specific angles to generate lateral and bird's-eye views of the cranial base.

For histology and immunohistochemistry, fixed skulls were rinsed in DEPC (diethyl pyrocarbonate)-treated water and decalcified in 0.1 M Tris, pH 7.5 buffer containing 0.1% DEPC, 10% EDTA-4 Na, and 7.5% polyvinyl pyrolidione (PVP). For routine histological analysis, 5 μm sections were stained with hematoxylin and Eosin or Fast green using standard procedures. To visualize primary cilia by immunofluorescence staining, 10 μm paraffin sections were incubated with a 1:200 dilution of anti-acetylated α-tubulin monoclonal antibody (Sigma, Clone 6-11B-1) followed by biotinylated secondary antibodies and Cy3-conjugated streptavidin (Vector Laboratories) to yield a signal. Sections were counterstained with YOPRO-3 iodide (612/631) or 4′,6-diamidino-2-phenylindole dihydrochloride (DAPI) (Invitrogen) to reveal nuclei. To visualize hedgehog protein distribution, paraffin sections were subjected to antigen retrieval by incubation in 0.05% citraconic anhydride pH 7.4 at 93°C for a total of 30 minutes (Namimatsu et al., 2005). Following blocking with 5% normal goat serum, sections were incubated with a 1:500 dilution of rabbit anti-mouse Shh (Ab80) in 5% normal goat serum at 4°C overnight; this antibody mixture had been pre-spun at 10,000 ***g*** at 4°C for 10 minutes prior to use. After overnight incubation, sections were rinsed in phosphate-buffered saline (PBS) and incubated with biotinylated goat anti-rabbit IgGs followed by Cy3-Streptavidin according to the manufacturer's recommendation. Nuclear counterstaining was carried out with diluted DAPI solution for 5 minutes at room temperature.

Gene expression analysis

Serial paraffin tissue sections were pretreated with 10 μg/ml proteinase K (Sigma) for 10 minutes at room temperature, post-fixed in 4% paraformaldehyde, washed with PBS containing 2 mg/ml glycine and treated with 0.25% acetic anhydride in triethanolamine buffer (Koyama et al., 1996). Sections were hybridized with antisense or sense ^{35}S-labeled probes [approximately 1×10^6 disintegrations per second (DPM)/section] at 50°C for 16 hours. Mouse cDNA clones included: histone H4C [nucleotides (nt.) 549-799; AY158963]; *Pthrp* (nt. 66-1386; NM_008970); osteopontin (*Spp1*; nt. 1-267; AF515708); *osterix* (*Sp7*; nt. 40-1727; NM_130458); *Vegf* (*Vegfa*; nt. 115-539; gi/249858); *Ihh* (nt. 897-1954; MN_010544); Patched 1 (*Ptch1*; nt.

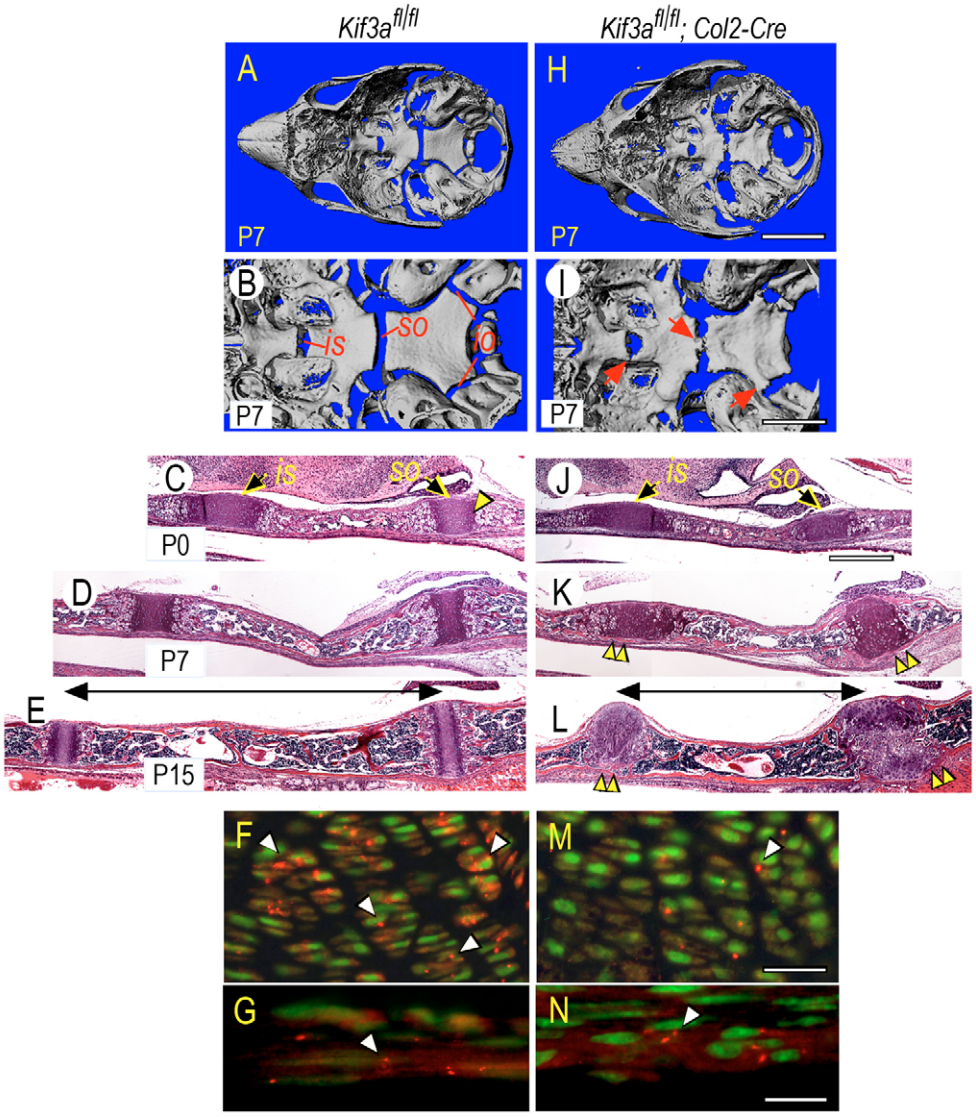

Fig. 1. *Kif3a*-deficient cranial bases and synchondroses are abnormal. (**A**,**B**,**H**,**I**) Skulls from P7 control (*Kif3a*$^{fl/fl}$; A,B) and *Kif3a*-deficient (*Kif3a*$^{fl/fl}$*;Col2-Cre*; H,I) mice were analyzed by micro-computed tomography (μCT) and are shown by birds-eye view at low (A,H) and high (B,I) magnification. The location of intrasphenoidal (*is*), spheno-occipital (*so*) and intra-occipital (*io*) synchondroses is indicated in controls (B); arrows point to defects in mutant specimens (I). (**C-E**,**J-L**) Parasagittal hematoxylin and Eosin (H&E)-stained sections of control (C-E) and *Kif3a*-deficient (J-L) cranial bases at P0, P7 and P15 displaying *is* and *so* synchondroses as well as intervening endochondral bone. Notice that the histology and organization of mutant synchondroses are markedly abnormal compared with controls, and that the distance between the synchondroses is also reduced (indicated by double-headed arrow). Arrowheads indicate ectopic bone formation. (**F**,**G**,**M**,**N**) Immunolocalization of acetylated α-tubulin in primary cilia (arrowheads) in P0 control (F,G) and *Kif3a*-deficient (M,N) synchondrosis growth plate and associated perichondrium. Scale bars: 5 mm in H for A,H; 2 mm in I for B,I; 300 μm in J for C-E and J-L; 100 μm in M for F,M; and 35 μm in N for G,N. *is*, intrasphenoidal; *io*, intra-occipital; P, postnatal day; *so*, spheno-occipital.

81-841; NM_008957); smoothened (nt. 450-1000; BC048091); collagen X (*Col10a1*; nt. 1302-1816; NM009925); and collagen II (*Col2a1*; nt. 1095-1344; X57982). After hybridization, slides were washed with 2× sodium chloride-sodium citrate buffer (SSC) containing 50% formamide at 50°C, treated with 20 μg/ml RNase A for 30 minutes at 37°C and washed three times with 0.1× SSC at 50°C for 10 minutes/wash. Sections were dehydrated with 70, 90 and 100% ethanol for 5 minutes/step, coated with Kodak NTB-3 emulsion diluted 1:1 with water, and exposed for 10-14 days. Slides were developed with Kodak D-19 at 20°C and stained with hematoxylin. Dark- and bright-field images were captured using a digital camera, and dark-field images were pseudo-colored using Adobe Photoshop software.

RESULTS

Cranial base and synchondroses are abnormal in conditional *Kif3a*-deficient mice

Gross anatomical inspection showed that the craniofacial skeleton was quite defective in *Kif3a*$^{fl/fl}$*;Col2a1-Cre* mice (hereafter termed *Kif3a*-deficient mice) compared with *Kif3a*$^{fl/wt}$*;Col2a1-Cre* and *Kif3a*$^{fl/fl}$ mice (hereafter termed control mice), particularly at postnatal stages. Thus, we processed the skulls of postnatal day (P)0, P7 and P15 mice for micro-computed tomography (μCT) and histology, focusing on the cranial base. Control cranial bases displayed a typical elongated morphology along the anteroposterior axis (Fig. 1A) and their intrasphenoidal (Fig. 1B, *is*), spheno-occipital (Fig. 1B, *so*) and intra-occipital (Fig. 1B, *io*) synchondroses were well-defined and distinct. Histologically, the synchondroses were fully cartilaginous, reflecting their active growth status, and flanked intervening regions of endochondral bone (Fig. 1C-E). By contrast, P7 *Kif3a*-deficient cranial bases were wider than controls (Fig. 1H), and their synchondroses were deformed (Fig. 1I) and even exhibited segments of mineralized tissue bridging the neighboring bones (Fig. 1I, arrows), a potentially catastrophic defect that would hamper growth. Their overall histological organization and shape were already defective at P0 (Fig. 1J), and much more so at P7 and P15 (Fig. 1K,L), and the length of the intervening bone region was markedly decreased (Fig. 1E,L, horizontal bars), reflecting the shortening of the cranial base along its anteroposterior axis. Immunostaining with antibodies to acetylated α-tubulin confirmed that primary cilia were obvious in control chondrocytes (Fig. 1F, arrowheads) but rare in *Kif3a*-deficient chondrocytes (Fig. 1M, arrowhead), attesting to the effectiveness of the action of *Col2a1-Cre*. In addition, primary cilia were equally evident in perichondrial tissue of both control and *Kif3a*-deficient cranial bases (Fig. 1G,N, arrowheads), attesting to the specificity of *Col2a1-Cre* action being clearly limited to cartilage.

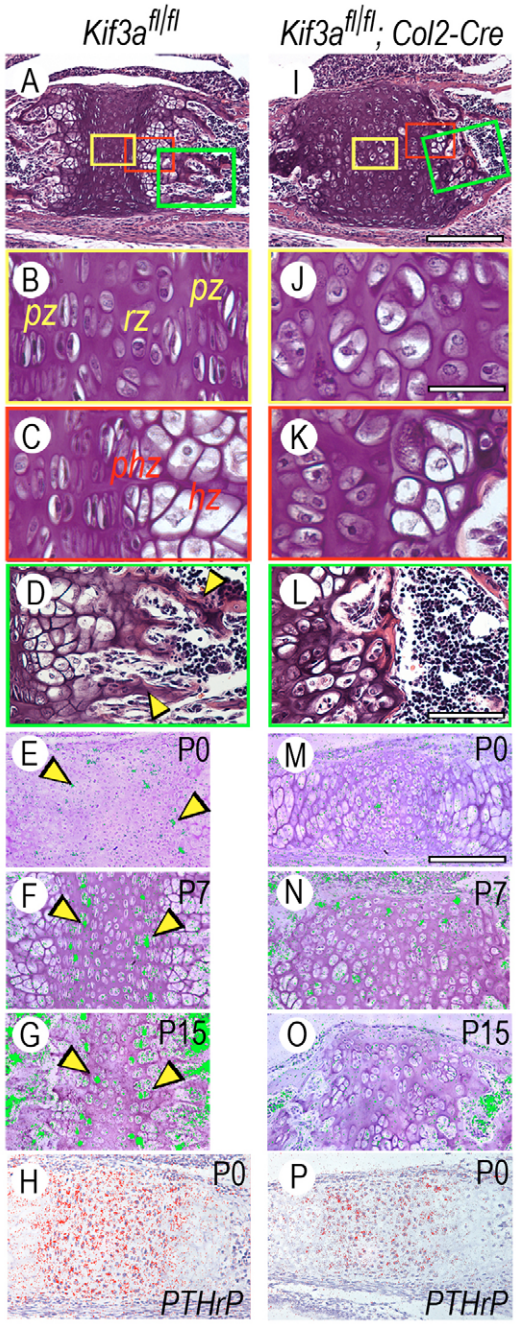

Fig. 2. Synchondrosis growth plate organization and chondrocyte proliferation are deranged in *Kif3a*-deficient cranial bases. (**A-D**) Parasagittal sections of a P7 control spheno-occipital synchondrosis. Notice the presence of resting (*rz*), proliferative (*pr*), pre-hypertrophic (*phz*) and hypertrophic (*hz*) growth plate zones and primary bone spongiosa (arrowheads in D). Areas in colored frames in A are shown at higher magnification in B-D. (**E-G**) Presence and location of proliferating chondrocytes in control P0 (E), P7 (F) and P15 (G) spheno-occipital synchondroses as revealed by histone 4C gene expression by in situ hybridization. The hybridization signal was given an artificial color for illustration purpose. Notice the presence of two well-defined proliferative zones (indicated by arrowheads) flanking a central resting zone. (**H**) *Pthrp* gene expression in a control P0 synchondrosis, which characterizes the resting and proliferative zones. (**I-L**) Parasagittal sections of a P7 *Kif3a*-deficient spheno-occipital synchondrosis showing that the growth plate zone structure is totally abnormal (J,K) and that there is a near absence of primary spongiosa (L). (**M-O**) Near absence of histone 4C-expressing proliferating chondrocytes in *Kif3a*-deficient synchondroses. (**P**) *Pthrp* gene expression in a *Kif3a*-deficient synchondrosis. Scale bars: 300 μm in I for A,I; 40 μm in J for B,C,J,K; 80 μm in L for D,L; and 150 μm in M for E-H and M-P. P, postnatal day; *rz/pr/phz/hz*, resting/proliferative/pre-hypertrophic/hypertrophic growth plate zones.

Gene expression analysis reveals dysfunction of mutant growth plates

Upon closer microscopic inspection, control synchondroses, such as the spheno-occipital synchondrosis (Fig. 2A), displayed characteristic growth plate zones of small, round, resting chondrocytes (Fig. 2B, *rz*); flat-shaped proliferating chondrocytes (Fig. 2B, *pz*); and oval pre-hypertrophic chondrocytes and large mature hypertrophic chondrocytes (Fig. 2C, *phz* and *hz*). The hypertrophic zone was followed by primary bone spongiosa intermixing with marrow (Fig. 2D, arrowheads). By sharp contrast, *Kif3a*-deficient growth plates lacked well-defined zones (Fig. 2I). In particular, small-sized resting chondrocytes and flat-shaped chondrocytes were conspicuously absent; instead, a mixed population of slightly enlarged and oval-to-round chondrocytes was present (Fig. 2J,K). In addition, the hypertrophic zone was very small (Fig. 2K) and there was an abrupt transition from cartilage to marrow, and a concurrent reduction in primary spongiosa and endochondral bone (Fig. 2L) (Xiao et al., 2006). In line with the absence of flat-shaped cells, mutant growth plates contained few proliferating chondrocytes, as indicated by gene expression of the mitotic marker histone 4C (Fig. 2M-O), whereas the cells were abundant and organized in two distinct proliferative zones in control growth plates (Fig. 2E-G, arrowheads). Indeed, gene expression of *Pthrp*, a major regulator of growth plate chondrocyte proliferation (Lanske et al., 1996; Vortkamp et al., 1996), was strong in controls (Fig. 2H), but was low in mutant growth plates (Fig. 2P).

Growth plate disorganization, and deficiency in primary spongiosa and endochondral bone suggested that the chondrocyte maturation process had been deranged in *Kif3a*-deficient synchondroses. In situ hybridization showed that, compared with controls, the mutant chondrocytes did display low and scattered expression of Ihh and collagen X (Col10a1), which are characteristic gene products of pre-hypertrophic and early hypertrophic chondrocytes (Fig. 3B,C,G,H), and expressed equally low levels of *MMP-13* (also known as *Mmp13* – Mouse Genome Informatics) and *Vegf* (*Vegfa*), which are important for cartilage-to-endochondral bone transition (Fig. 3D,E,I,J) (Engsig et al., 2000; Zelzer et al., 2002). Deficiency in primary spongiosa (Fig. 4F) was reflected in the fact that expression of such bone markers and regulators as osteopontin (also known as *Spp1* – Mouse Genome Informatics), collagen I (*Col1a1*), *Runx2* and osterix (also known as *Sp7* – Mouse Genome Informatics) was quite low in mutant (Fig. 4G-J) versus control (Fig. 4B-E) specimens. Despite all of these serious changes, mutant chondrocytes still exhibited strong collagen II (*Col2a1*) gene expression, as did controls (Fig. 3A,F), signifying that the basic differentiated phenotype in mutants was largely preserved.

Excessive intramembranous ossification and ectopic cartilage formation

As they develop and mature in the growth plate, pre-hypertrophic and hypertrophic chondrocytes induce the formation of intramembranous bone in adjacent perichondrial tissues, a process that is attributable to *Ihh* expression (Koyama et al., 1996; Nakamura et al., 1997;

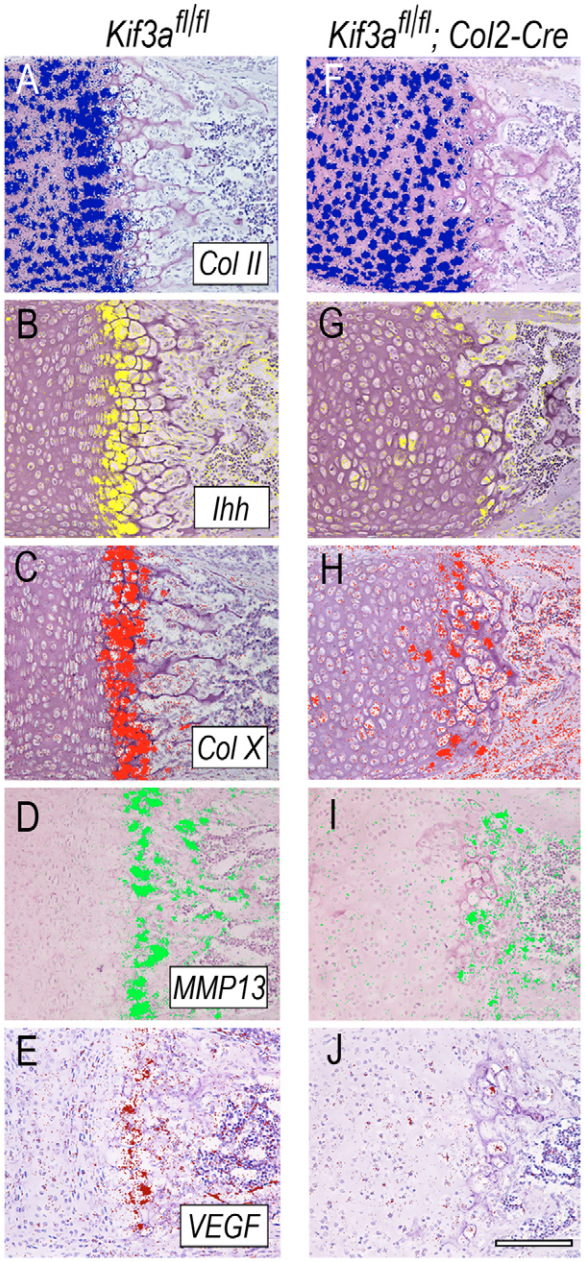

Fig. 3. Gene expression of chondrocyte-maturation-associated genes is depressed in *Kif3a*-deficient synchondroses. Serial sections from the medial portion of P7 control (**A-E**) and *Kif3a*-deficient (**F-J**) spheno-occipital synchondroses were processed for in situ hybridization analysis of the indicated genes, using radiolabeled riboprobes. The hybridization signal was given artificial colors and images were superimposed with hematoxylin histologic images of the corresponding field. Scale bar: 100 μm in J for for A-J.

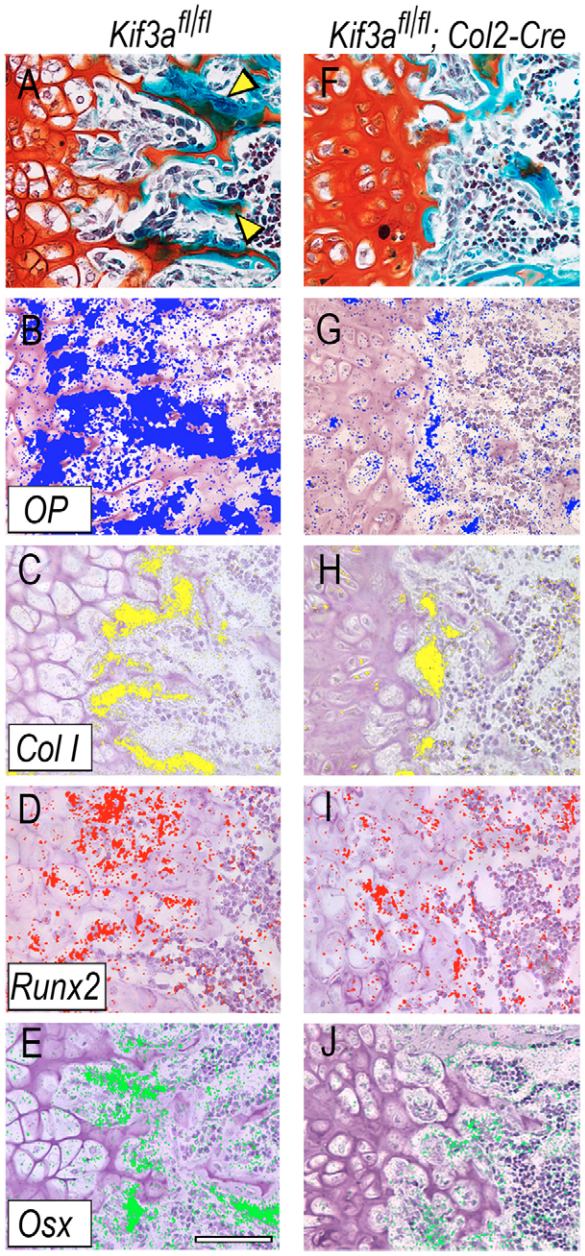

Fig. 4. Gene expression of cartilage-to-bone-associated genes and the formation of primary spongiosa are inhibited in *Kif3a*-deficient synchondroses. (**A**,**F**) Parasagittal serial sections of P7 control (A) and mutant (F) spheno-occipital synchondrosis were stained with fast green/Safranin O to reveal bone tissue (dark blue). Notice the marked reduction of primary bone spongiosa in mutant tissue (F), which is highly visible in controls (A, arrowheads). (**B-E**,**G-J**) Expression of the indicated genes as revealed by in situ hybridization with serial sections of control (B-E) and mutant (G-J) tissue. The hybridization signal was given artificial colors and images were superimposed with hematoxylin histologic images of the corresponding field. Scale bar: 80 μm in E for A-J.

St-Jacques et al., 1999). Control synchondroses, such as the spheno-occipital synchondrosis, conformed to this general rule. It displayed fast-green-positive intramembranous bone flanking the Ihh-rich pre-hypertrophic and hypertrophic zones (Fig. 5A, arrowhead), and which expressed collagen I, *Runx2* and osterix (Fig. 5B-D, arrowheads); importantly, there was no appreciable bone flanking the proliferative and resting zones, as was to be expected (Fig. 5A-D, arrows). By contrast, intramembranous bone had formed all along the growth plate in companion *Kif3a*-deficient synchondrosis, thus spanning the entire flank of the synchondrosis and bridging the neighboring occipital and

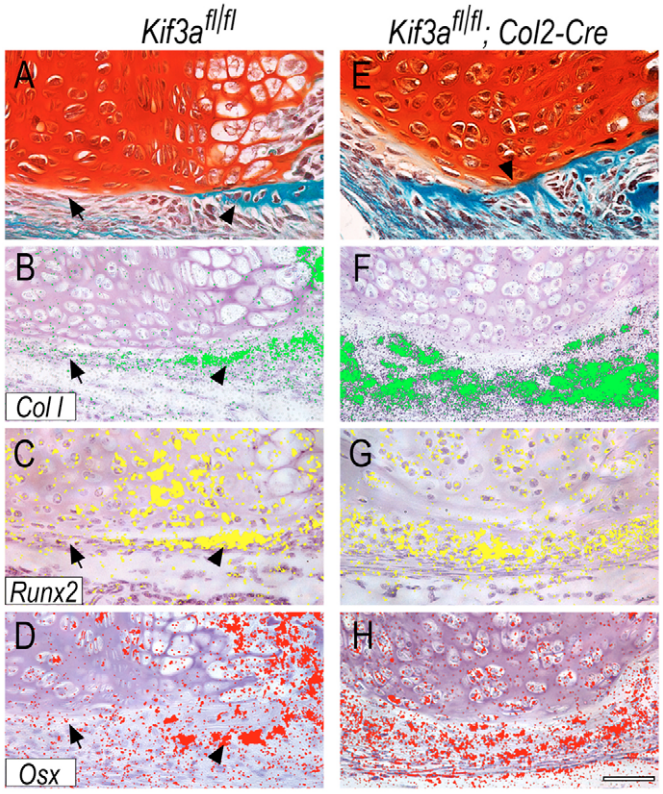

Fig. 5. Intramembranous ossification is excessive near *Kif3a*-deficient synchondroses. Parasagittal serial sections of P7 control (**A-D**) and mutant (**E-H**) spheno-occipital synchondroses were processed for staining with fast green/Safranin O (A,E) or in situ hybridization analysis of the indicated genes (B-D,F-H). (A-D) In controls, notice the presence of the intramembranous bone collar adjacent to the pre-hypertrophic and hypertrophic zones (arrowheads) and its absence near the proliferative and resting zones (arrows), as is to be expected. Notice instead that the intramembranous bone had formed all along the flank of the *Kif3a*-deficient synchondrosis (E-H). Scale bar: 75 μm in H for A-H.

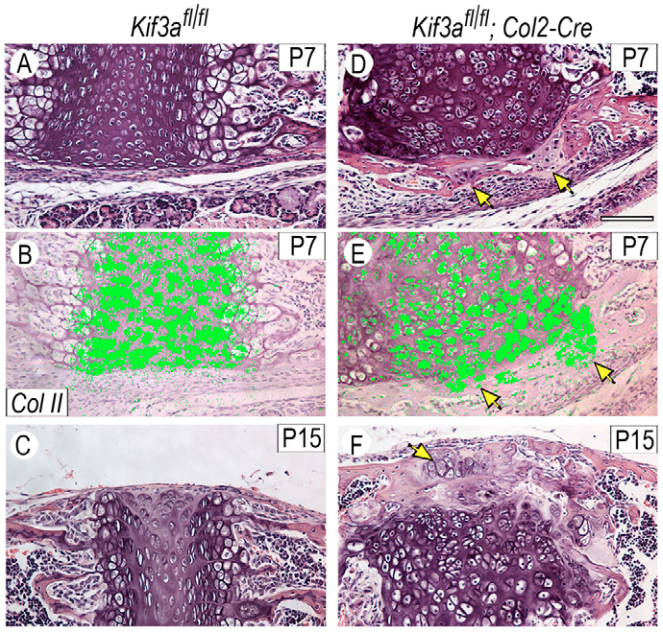

Fig. 6. Presence of ectopic cartilage masses near *Kif3a*-deficient synchondroses. Sections of P7 and P15 control (**A-C**) and mutant (**D-F**) synchondroses were stained with hematoxylin and Eosin (H&E) or processed for in situ hybridization analysis of collagen II expression. Ectopic cartilaginous masses forming in mutant specimens (arrows in D-F) are recognizable by their typical histology and expression of collagen II. Such a phenomenon is never observed in control specimens, in which the chondro-perichondrial boundary is clear and unviolated (A-C). Scale bar: 75 μm in D for A-F.

sphenoidal bones (Fig. 5E-H). This excess intramembranous bone undoubtedly corresponds to the regions of mineralized tissue initially detected by μCT (Fig. 1I, arrows) and appreciable also by general histology (Fig. 1K,L, double arrowheads).

Based on these findings, we asked whether there might be additional aberrations occurring in perichondrial tissues flanking *Kif3a*-deficient synchondroses. Further scrutiny did reveal that, surprisingly, ectopic cartilage masses had formed at several sites (Fig. 6D-F, arrows). The tissue was recognizable by its characteristic histology as well as collagen II gene expression and was located almost invariably in close proximity to the mutant synchondrosis growth plates (Fig. 6D-F, arrows), thus displaying a topographical arrangement also seen in pathological exostoses that form in close proximity to growth plates (Hecht et al., 1995). Ectopic cartilage masses were never seen in tissues flanking control synchondroses, and their chondro-perichondrial boundary was extremely well-defined and un-violated (Fig. 6A-C).

Aberrant topography of hedgehog signaling

What could have triggered excessive intramembranous ossification and ectopic cartilage formation near mutant growth plates? An obvious possibility was that hedgehog signaling, and in particular the topography of signaling, had changed in mutant specimens, triggering broader responses in neighboring perichondrial tissues. To test this possibility, we determined the expression patterns of *Ihh* and of its target genes Patched 1 and *Gli1* in control and *Kif3a*-deficient synchondroses. We chose to focus on P0, hoping to detect changes in signaling patterns as early as possible. In controls, the three genes displayed predictable and distinct expression patterns, with abundant *Ihh* transcripts in pre-hypertrophic zones (Fig. 7A,B,G,H, *phz*) and Patched 1 and *Gli1* transcripts in preceding proliferative zones (Fig. 7C,D,I,J, *pz*), reflecting the well-established and direct role of Ihh in chondrocyte proliferation (Shimo et al., 2004; St-Jacques et al., 1999). There was also clear Patched 1 and *Gli1* expression in perichondrial tissue flanking the pre-hypertrophic and hypertrophic zones where the intramembranous bone collar normally forms (Fig. 7C,D,I,J, single arrowhead), but perichondrium flanking the resting and proliferative zones was negative (Fig. 7C,D,I,J, double arrowhead). Smoothened transcripts were present throughout the growth plates (Fig. 7E,K). In mutant synchondroses, *Ihh* expression was still appreciable at this stage (Fig. 7M,N,S,T). However, expression of both Patched 1 and *Gli1* was markedly decreased and the transcripts were scattered within the growth plates (Fig. 7O,P,U,V), signifying that hedgehog signaling was feeble and diffuse. On the other hand, the Patched 1 and *Gli1* transcripts were actually quite evident along the entire length of perichondrial tissues (Fig. 7O,P,U,V, arrowhead), thus closely mirroring the location of excessive intramembranous bone formation. Smoothened expression was largely unaffected (Fig. 7Q,W). Immunohistochemistry showed that Ihh distribution in the mutants had also been re-arranged. In controls, the protein was abundant in pre-hypertrophic chondrocytes,

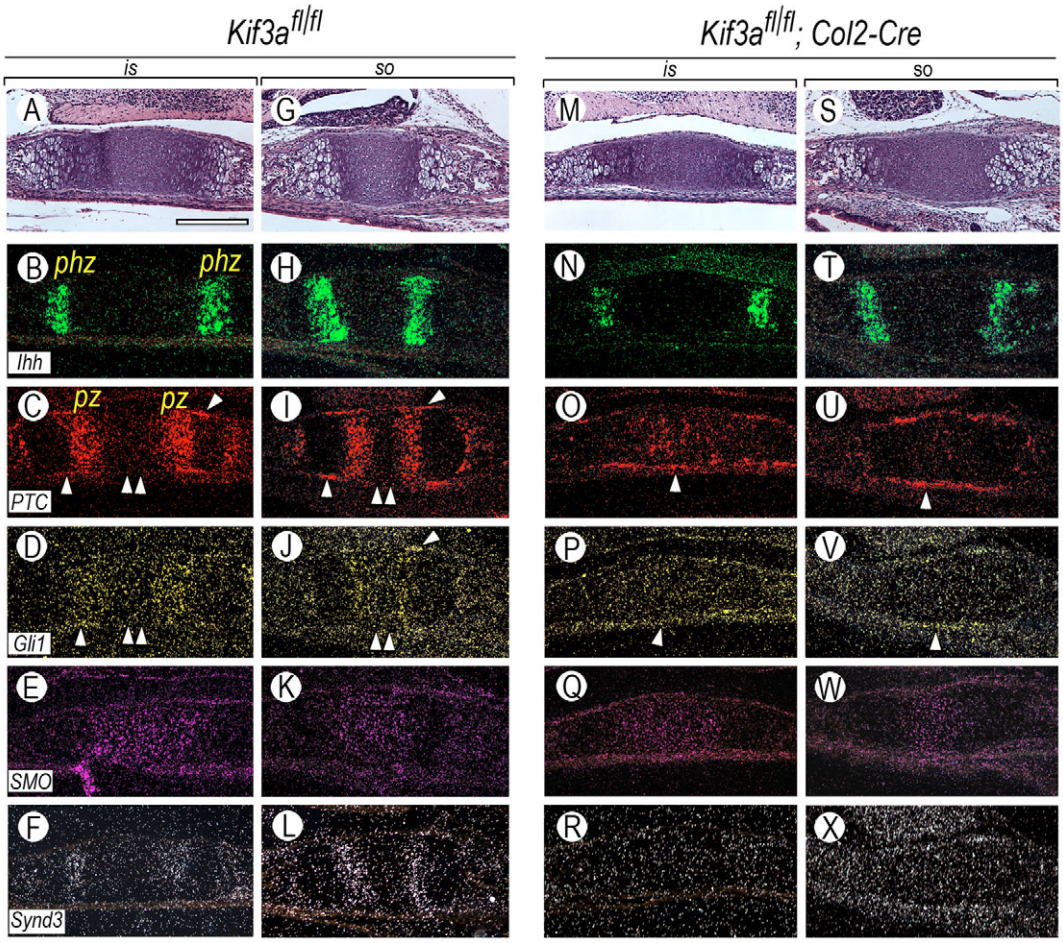

Fig. 7. Topography of hedgehog signaling is altered in *Kif3a*-deficient synchondroses. Serial sections of P0 control (**A-L**) and mutant (**M-X**) intrasphenoidal (*is*) and spheno-occipital (*so*) synchondroses were processed for expression analysis of the indicated genes. (C,D,I,J) Notice that, in controls, Patched 1 (C,I) and *Gli1* (D,J) were expressed in the proliferative zone (*pz*) and in the perichondrium flanking the pre-hypertrophic and hypertrophic zones (single arrowheads), but not in the perichondrium flanking the resting and proliferative zones (double arrowheads). (O,P,U,V) In mutants, however, Patched 1 (O,U) and *Gli1* (P,V) are minimally expressed within the growth plates, but are expressed all along the perichondrial tissues (arrowheads). (F,L,R,X) Notice also that syndecan 3 gene expression is mainly restricted to the proliferative zone in controls (F,L), but is extremely low in mutants (R,X). Expression of *Ihh* and smoothened was similar in control (B,H,E,K) and mutant (N,T,Q,W) tissues at this stage. *is*, intrasphenoidal; *pz*, proliferative zone; *so*, spheno-occipital. Scale bar: 150 μm in A for A-X.

as well as in neighboring proliferative chondrocytes and in the inner perichondrial layer (Fig. 8A,B, arrowhead), and was undetectable in the upper growth plate region and flanking perichondrium (Fig. 8B, double arrowhead) as expected (Yin et al., 2002). In the mutants, Ihh formed a much more expansive gradient that extended throughout the upper growth plate region and along the entire length of perichondrium (Fig. 8C,D, double arrowhead). Specificity of staining was reaffirmed by the fact that sections from *Ihh*-null mice were negative (Fig. 8E,F).

To reinforce the idea that the control of hedgehog signaling topography was altered in mutant synchondroses, we assessed whether the expression of molecules needed to direct and restrict hedgehog signaling was altered as well. We focused on heparan sulfate proteoglycans known for their pivotal roles in hedgehog signaling logistics (Bellaiche et al., 1998; The et al., 1999), and on syndecan 3 in particular, which we found to participate in such roles in long bone growth plates (Shimazu et al., 1996; Shimo et al., 2004). In controls, the syndecan 3 gene was expressed in the proliferative zones of synchondrosis growth plates (Fig. 7F,L) along with Patched 1 and *Gli1*, in line with the idea that this syndecan may aid and delimit Ihh action on chondrocyte proliferation (Pacifici et al., 2005). However, there was barely detectable syndecan 3 gene expression in *Kif3a*-deficient synchondroses (Fig. 7R,X).

Skeletal aberrations are caused by postnatal *Ihh* deficiency

The severe cranial base and synchondrosis abnormalities triggered by *Kif3a* deficiency in cartilage raised the issue of whether they had a unique character or whether they would resemble those elicited by a deficiency in related genes, such as *Ihh*. Accordingly, we created conditional postnatal mice lacking *Ihh* in cartilage by treating neonatal $Ihh^{fl/fl}$*;Col2a-CreER* mice with tamoxifen. Mice were sacrificed at P7 and P15 (hereafter termed *Ihh*-deficient mice); neonatal $Ihh^{fl/fl}$ littermates were treated with tamoxifen in parallel and served as controls. *Ihh*-deficient skulls exhibited anteroposterior shortening and abnormal synchondroses (Fig. 9E) relative to controls (Fig. 9A), reminiscent of the defects seen in *Kif3a*-deficient skulls, described above. At variance with the latter, however, the

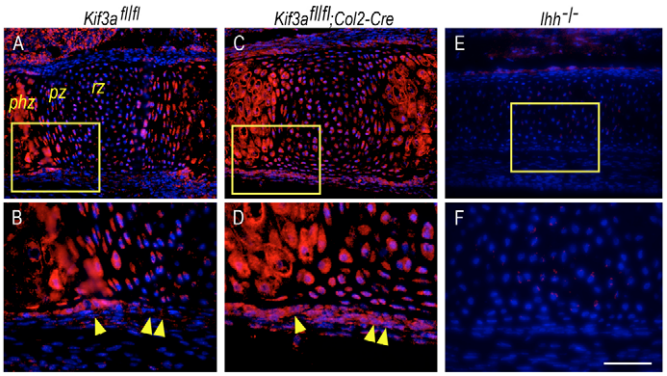

Fig. 8. Ihh distribution is altered in *Kif3a*-deficient synchondroses. (**A-D**) Serial sections of P0 control (A,B) and *Kif3a*-deficient (C,D) spheno-occipital synchondroses were processed for immunohistochemistry using Ab80 rabbit hedgehog antibodies. Sections were reacted with secondary fluorescent antibodies and counterstained with the nuclear dye DAPI (blue). Positive immunosignal is orange in color. (A,B) In controls, Ihh is present in the pre-hypertrophic zone (*phz*) and in adjacent proliferative chondrocytes and inner perichondrium (B, single arrowhead), but is undetectable in the upper growth plate zones and flanking perichondrium (B, double arrowhead). (C,D) However, in *Kif3a*-deficient specimens, Ihh is present in a more extensive and expansive gradient form throughout much of growth plate and all along perichondrium (D, single and double arrowheads). (**E**,**F**) Notice that the hedgehog antibodies produced no detectable signal with sections from *Ihh*-null synchondroses, attesting to their specificity. (B,D,F) Higher-magnification images of the boxed area in A,C and E, respectively. *rz/pr/phz*, resting/proliferative/pre-hypertrophic growth plate zones. Scale bar: 65 μm in F for B,D,F.

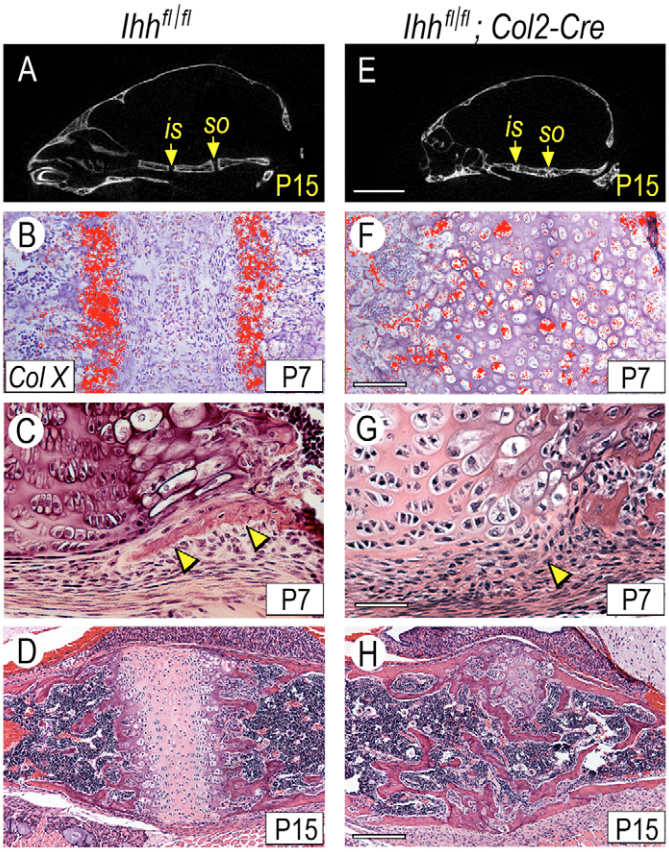

Fig. 9. Conditional postnatal *Ihh* deficiency causes cranial base abnormalities. (**A**,**E**) Skulls from P15 control (A) and *Ihh*-deficient (E) mice were subjected to micro-computed tomography (μCT) analysis; one orthogonal plane through the cranial base of each is shown here. Notice the presence of well-defined intrasphenoidal (*is*) and spheno-occipital (*so*) synchondroses in controls (A), and the ill-defined synchondroses and reduced anteroposterior length in mutants (E). (**B-D**,**F-H**) Sections from P7 and P15 control (B-D) and mutant (F-H) *so* synchondroses processed for collagen X gene expression (B,F) or for histological analysis (C,D,G,H). Notice that collagen X transcripts (red) are restricted to hypertrophic zones in controls (B) but are widespread throughout the mutant synchondrosis (F). Notice also the presence of a well-formed intramembranous bone collar flanking the pre-hypertrophic and hypertrophic zones in controls (C, arrowheads), which is undetectable in mutants (G, arrowhead). (D,H) Additionally, in mutants, much of the synchondrosis is replaced by endochondral bone by P15 (H). *is*, intrasphenoidal; *so*, spheno-occipital. Scale bar: 2 mm in E for A,E; 150 μm in F for B,F; 75 μm in G for C,G; and 250 μm in H for D,H.

Ihh-deficient growth plates were entirely occupied by collagen X-expressing hypertrophic chondrocytes (Fig. 9F) and there was no detectable intramembranous ossification in the flanking perichondrial tissues (Fig. 9G, arrowhead) relative to controls (Fig. 9B,C). Defects were exacerbated by P15, at which point much of the *Ihh*-deficient synchondroses had been replaced by endochondral bone and marrow, and remnants of growth plate tissue were confined to a lateral and inconspicuous position (Fig. 9H), phenomena not seen in P15 *Kif3a*-deficient specimens.

Discussion

In this study, we provide evidence that Kif3a and primary cilia are pivotal for cranial base and synchondrosis development and function. *Kif3a* deficiency alters the anteroposterior and lateral growth patterns of the cranial base, resulting in skull dysmorphogenesis that is reminiscent of defects seen in some Aperts and Crouzon patients (Kreiborg et al., 1993). *Kif3a* deficiency affects, as severely, the behavior and functional organization of synchondrosis growth plates, resulting in a quasi-stasis of the chondrocyte maturation process and retardation of endochondral bone formation. Concurrently, there were unexpected and unpredicted alterations in developmental events occurring in synchondrosis perichondrial tissues, including excessive intramembranous ossification – most likely impacting very negatively on cranial base growth. Only some of these defects resembled those caused by a conditional deficiency of *Ihh*, indicating that Kif3a and primary cilia make unique contributions to the normal progression of cranial base and synchondrosis development, organization and function.

Growth plates are complex multi-facet structures in which chondrocyte shape, orientation and polarity, chondrocyte proliferation and phenotype, and chondrocyte maturation and hypertrophy must all be regulated in a coordinated manner. A well-established mechanism delineated by work on developing long bones is the PTHrP-Ihh axis, in which PTHrP produced by periarticular cells under the influence of Ihh regulates the rate of chondrocyte proliferation (Lanske et al., 1996). In line with this model, *Ihh* gene ablation in mouse embryos causes the downregulation of *Pthrp* expression and reduced proliferation (St-Jacques et al., 1999). This mechanism can certainly account for the decrease in chondrocyte proliferation in *Kif3a*-deficient growth

plates, which express low if any PTHrP. This would imply that synchondroses conform to, and obey, the PTHrP-Ihh axis (Young et al., 2006) and that a normal complement of Kif3a and primary cilia is needed to maintain this axis. Reduced proliferation was accompanied by the absence of flat-shaped chondrocytes, which normally constitute the proliferative zone; by the absence of distinct resting, pre-hypertrophic and hypertrophic zones; and by the absence of a columnar cell organization. Such nearly chaotic organization of *Kif3a*-deficient growth plates thus suggests that the mutant chondrocytes may lack key topographical, navigational or mechanical mechanisms and devices that enable them to perceive location or cues within the growth plate and adopt appropriate zone-specific polarity, shape and phenotype. One such mechanism could be the planar cell polarity pathway (PCP), a form of non-canonical Wnt pathway mediated by primary cilia that is essential for cell orientation and mitotic spindle alignment in organs such as the inner ear, kidney tubules and cranial cartilage (Dabdoub and Kelley, 2005; Fischer et al., 2006; Park et al., 2006). The importance and centrality of the PCP pathway in several systems make it likely that it operates in growth plates as well (Olsen et al., 2005), where it could orient the chondrocyte mitotic spindle and division plane, which are usually perpendicular to the longitudinal axis of the growth plate (Dodds, 1930), or where it could promote the related process of columnar organization. Notably, because both the PCP pathway and hedgehog proteins act via primary cilia, chondrocytes could control their own polarity and orientation in relation to, and in correlation with, their responses to Ihh, which is distributed in the form of gradients within the growth plate (Gritli-Linde et al., 2001; Koziel et al., 2004; Yin et al., 2002).

In addition to being disorganized, *Kif3a*-deficient growth plates exhibited a severe delay in chondrocyte maturation and hypertrophy and were occupied by oval-to-round chondrocytes expressing the collagen II gene but little if any maturation genes, including collagen X and *Vegf*, and were followed by a poor primary bone spongiosa. These phenotypic defects are rather unusual and are clearly different from those seen in prenatal *Ihh*-null synchondroses (Young et al., 2006) or in the postnatal *Ihh*-deficient synchondroses described here in which there is exuberant and widespread chondrocyte hypertrophy followed by endochondral bone. One possibility is that the *Kif3a*-deficient chondrocytes are unable to respond to factors that regulate their maturation and hypertrophy, including β-catenin-dependent Wnt proteins (Enomoto-Iwamoto et al., 2002; Mak et al., 2006; Tamamura et al., 2005), the signaling and action of which may involve primary cilia (Germino, 2005). Alternatively, the topographical disorganization discussed above could have led to general intermingling and intermixing of chondrocytes with different phenotypic properties and maturation status within the mutant growth plates, creating conditions in which the cells interfere with the phenotype of each other. Previously, we showed that, when immature chondrocytes are co-cultured with hypertrophic chondrocytes, the hypertrophic phenotype is suppressed (D'Angelo and Pacifici, 1997). It is important to note and discuss here the findings recently described by Haycraft et al. (Haycraft et al., 2007). These authors suggested that chondrocyte hypertrophy was accelerated in the long bone anlagen of *prx1cre;Ift88* or *prx1cre;Kif3a* mouse embryo limbs, based on histological measurements of growth plate zones. These findings would appear to be in sharp contrast to the severe delay in chondrocyte hypertrophy that we observe in our *col2cre;Kif3a* synchondroses, but there are several plausible explanations for these apparent differences. One is that the developmental consequences of a broad deletion of primary cilia function by *prx1cre* may differ from those

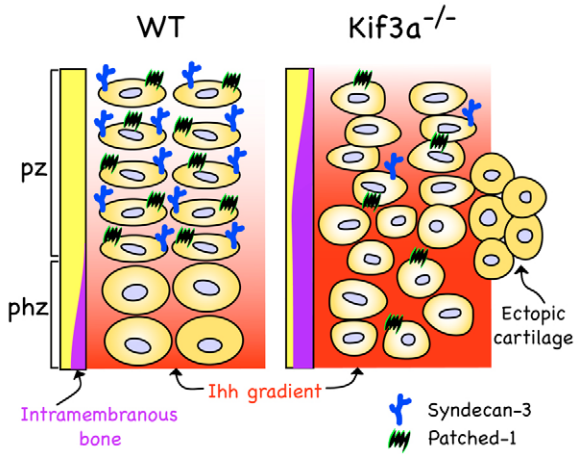

Fig. 10. Model illustrating the phenotypic consequences of *Kif3a* deficiency. In a wild-type (WT) synchondrosis growth plate, Ihh would produce a physiologically restricted gradient (red) from the pre-hypertrophic zone (phz) into the flanking perichondrium and the preceding proliferative zone (pz). The upper limit of this restricted field of action would be set by Patched 1 and syndecan 3 (and other heparan sulfate proteoglycans), and would allow the normal proliferation of chondrocytes and the normal formation of intramembranous bone. In *Kif3a*-deficient (*Kif3a*$^{-/-}$) growth plates, however, the Ihh distribution gradient would be expanded because of the marked reduction of syndecan 3 and Patched 1 expression. As a consequence, the topography of hedgehog signaling and action would be altered as well. Within the growth plate, Ihh signaling would be feeble, causing abnormal behavior of chondrocytes. In perichondrial tissues, Ihh signaling would be abnormally high and widespread, triggering excessive intramembranous bone deposition and ectopic cartilage formation. phz, pre-hypertrophic zone; pz, proliferative zone; WT, wild type.

elicited by the more targeted cartilage-specific approach we use here. A second intriguing possibility is that the overall roles of primary cilia in developing long bones may somewhat differ from those in the cranial base. Third, Haycraft et al. did not use the several markers of chondrocyte maturation and hypertrophy and endochondral ossification that we use in our study, and effects on chondrocyte maturation and hypertrophy may have been underestimated. Lastly, some differences could reflect the fact that prenatal stages were examined in that study, whereas we focused on neonatal and early postnatal stages.

One of the most intriguing and unexpected defects seen in *Kif3a*-deficient synchondroses is the formation of excessive intramembranous bone and ectopic cartilage masses, which are both readily appreciable by P7. These defects are preceded by alteration in hedgehog-signaling topography, which is delineated by Patched 1 and *Gli1* expression along the entire length of perichondrial tissues. Given that hedgehog proteins can stimulate osteogenesis and chondrogenesis (Enomoto-Iwamoto et al., 2000; Nakamura et al., 1997), excess hedgehog signaling in perichondrial tissues could have directly caused excessive intramembranous bone and cartilage formation. What remains unclear, however, is why there is excess signaling all along the perichondrium to begin with, particularly starting at P0 when *Ihh* expression is still confined to fairly restricted growth plate zones (see Fig. 7). One possibility is that the excess signaling is an autonomous local response of the perichondrium to phenotypic defects in the adjacent growth plates. Alternatively, it

could be due to the mutant chondrocytes themselves. For example, *Kif3a*-deficient chondrocytes may lack means to control the location and distribution of Ihh, allowing it to diffuse broadly, form a more extensive gradient, reach the entire length of the perichondrium, and trigger excessive cartilage and bone formation. This scenario and chain of events (summarized in our model in Fig. 10) are sustained by our observation that *Kif3a*-deficient growth plates express little, if any, (a) Patched 1, which sequesters and restricts hedgehog signaling to target fields (Jeong and McMahon, 2004) or (b) syndecan 3, a component of heparan sulfate proteoglycan-based mechanisms limiting and restricting hedgehog diffusion and action in growth plates or other structures (Callejo et al., 2005; Koziel et al., 2004; Shimo et al., 2004).

In this regard, it is interesting to point out a recent study involving mice lacking one allele of *Ext2*, a Golgi-associated glycosyltransferase needed for heparan sulfate synthesis (Stickens et al., 2005). *Ext2* heterozygous mice were found to be deficient in heparan sulfate and exhibited ectopic cartilaginous masses near their growth plates, thus mimicking exostoses present in hereditary multiple exostosis (HME) patients, who often have *EXT2* or *EXT1* mutations and reduced heparan sulfate levels (Hecht et al., 1995). The exact link between heparan sulfate deficiency and exostosis formation is still poorly understood. In the *Ext2* study above, it was proposed that heparan sulfate deficiency reduces fibroblast growth factor (FGF) signaling and tilts the balance in favor of BMP signaling, resulting in chondrocyte misbehavior, weakening of the bone collar and formation of exostosis masses (Stickens et al., 2005). Our data, showing reduced syndecan 3 expression in the growth plate and excess hedgehog signaling and protein in flanking perichondrial tissues, point to hedgehog proteins and defective Kif3a-related mechanisms as culprits in exostosis formation as well. A similar role for hedgehog protein in exostosis formation was proposed in a study of mouse embryos bearing an *Ext1* hypomorphic mutation (Koziel et al., 2004). We do not know, however, how *Kif3a* deficiency and lack of primary cilia lead to a reduction in syndecan 3 expression. In previous studies, we did find that syndecan 3 overexpression in vivo and in vitro causes excess and widespread *Ihh* expression, suggesting that the two genes are coordinated and that such coordination may have been disrupted by *Kif3a* deficiency (Pacifici et al., 2005; Shimo et al., 2004). It is also possible that the reduction in syndecan 3 expression is independent of *Kif3a* deficiency, but both of these effects would contribute to the phenotype. Whatever the explanation, it will be interesting to clarify whether *Kif3a* deficiency also affects the expression of syndecan 4 and syndecan 2, which are normally expressed in the proliferative zone and perichondrial tissues, respectively (David et al., 1993; Pacifici et al., 2005), and/or expression of other heparan sulfate proteoglycans, including glypicans and perlecan. Given that hedgehog proteins, bone morphogenetic protein (BMPs), FGFs and Wnts are all heparan sulfate-binding factors (Bernfield et al., 1999), the data may provide insights into how the various heparan sulfate proteoglycans, with their distinct binding specificity and expression patterns (Esko and Selleck, 2002), may help to mediate and coordinate the functions of the many signaling factors and pathways that converge to orchestrate the progression of skeletal development and how defects in these circuits could cause pathologies, including HME.

We thank C. J. Haycraft and B. K. Yoder (University of Alabama) and C. Farnum (Cornell University) for helpful discussions and suggestions during the course of the study. We are also grateful to A. P. McMahon (Harvard University) and A. Gritli-Linde (Goteborg University) for generously providing the Ab80 hedgehog antibodies. This work was supported by grants AR047543, AR046000 and AR050560 from the NIH.

References

Ansley, S. J., Badano, J. L., Blacque, O. E., Hill, J., Hoskins, B. E., Leitch, C. C., Kim, J. C., Ross, A. J., Eichers, E. R., Teslovich, T. M. et al. (2003). Basal body dysfunction is a likely cause of pleiotropic Bardet-Biedl syndrome. *Nature* **425**, 628-633.

Bellaiche, Y., The, I. and Perrimon, N. (1998). Tout-velu is a Drosophila homologue of the putative tumor suppressor EXT-1 and is needed for Hh diffusion. *Nature* **394**, 85-88.

Bernfield, M., Gotte, M., Park, P. W., Reizes, O., Fitzgerald, M. L., Lincecum, J. and Zako, M. (1999). Functions of cell surface heparan sulfate proteoglycans. *Annu. Rev. Biochem.* **68**, 729-777.

Bitgood, M. J. and McMahon, A. P. (1995). Hedgehog and Bmp genes are coexpressed at many diverse sites of cell-cell interaction in the mouse embryo. *Dev. Biol.* **172**, 126-138.

Callejo, A., Torroja, C., Quijada, L. and Guerrero, I. (2005). Hedgehog lipid modifications are required for hedgehog stabilization in the extracellular matrix. *Development* **133**, 471-483.

Chen, L., Adar, R., Yang, X., Monsonego, E. O., Cuiling, L., Hauschka, P. V., Yayon, A. and Deng, C.-X. (1999). Gly369Cys mutation in mouse FGFR3 causes achrondroplasia by affecting both chondrogenesis and osteogenesis. *J. Clin. Invest.* **104**, 1517-1525.

Corbit, K. C., Aanstad, P., Singla, V., Norman, A. R., Stainier, D. Y. R. and Reiter, J. F. (2005). Vertebrate Smoothened functions at the primary cilium. *Nature* **437**, 1018-1021.

D'Angelo, M. and Pacifici, M. (1997). Articular chondrocytes produce factors that inhibit maturation of sternal chondrocytes in serum-free agarose cultures: a TGFβ independent process. *J. Bone Miner. Res.* **12**, 1368-1377.

Dabdoub, A. and Kelley, M. W. (2005). Planar cell polarity and a potential role for a Wnt morphogen gradient in stereociliary bundle orientation in the mammalian inner ear. *J. Neurobiol.* **64**, 446-457.

Davenport, J. R. and Yoder, B. K. (2005). An incredible decade for the primary cilium: a look at a once-forgotten organelle. *Am. J. Physiol. Renal Physiol.* **289**, F1159-F1169.

David, G., Bai, X. M., Van der Schueren, B., Marynen, P., Cassiman, J.-J. and Van den Berghe, H. (1993). Spatial and temporal changes in the expression of fibroglycan (syndecan-2) during mouse embryonic development. *Development* **119**, 841-854.

Dodds, G. S. (1930). Row formation and other types of arrangement of cartilage cells in endochondral ossification. *Anat. Rec.* **46**, 385-399.

Engsig, M. T., Chen, Q.-J., Vu, T. H., Pedersen, A.-C., Therkidsen, B., Lund, L. R., Henriksen, K., Lenhard, T., Foged, N. T., Werb, Z. et al. (2000). Matrix metalloproteinase 9 and vascular endothelial growth factor are essential for osteoclast recruitment into developing long bones. *J. Cell Biol.* **151**, 879-889.

Enomoto-Iwamoto, M., Nakamura, T., Aikawa, T., Higuchi, Y., Yuasa, T., Yamaguchi, A., Nohno, T., Noji, S., Matsuya, T., Kurisu, K. et al. (2000). Hedgehog proteins stimulate chondrogenic cell differentiation and cartilage formation. *J. Bone Miner. Res.* **15**, 1659-1668.

Enomoto-Iwamoto, M., Kitagaki, J., Koyama, E., Tamamura, Y., Wu, C., Kanatani, N., Koike, T., Okada, H., Komori, T., Yoneda, T. et al. (2002). The Wnt antagonist Frzb-1 regulates chondrocyte maturation and long bone development during limb skeletogenesis. *Dev. Biol.* **251**, 142-156.

Esko, J. D. and Selleck, S. B. (2002). Order out of chaos: assembly of ligand binding sites in heparan sulfate. *Annu. Rev. Biochem.* **71**, 435-471.

Fischer, E., Legue, l., Doyen, A., Nato, F., Nicolas, J.-F., Torres, V., Yaniv, M. and Pontoglio, M. (2006). Defective planar cell polarity in polycystic kidney disease. *Nat. Genet.* **38**, 21-23.

Germino, G. G. (2005). Linking cilia to Wnts. *Nat. Genet.* **37**, 455-457.

Gritli-Linde, A., Lewis, P., McMahon, A. P. and Linde, A. (2001). The whereabouts of a morphogen: direct evidence for short- and graded long-range activity of hedgehog signaling peptides. *Dev. Biol.* **236**, 364-386.

Haycraft, C. J., Banizs, B., Aydin-Son, Y., Zhang, Q., Michaud, E. J. and Yoder, B. K. (2005). Gli2 and Gli3 localize to cilia and require intraflagellar transport protein Polaris for processing and function. *PLoS Genet.* **1**, 480-488.

Haycraft, C. J., Zhang, Q., Song, B., Jackson, W. S., Detloff, P. J., Serra, R. and Yoder, B. K. (2007). Intraflagellar transport is essential for endochondral bone formation. *Development* **134**, 307-316.

Hecht, J. T., Hogue, D., Strong, L. C., Hansen, M. F., Blanton, S. H. and Wagner, H. (1995). Hereditary multiple exostosis and chondrosarcoma: linkage to chromosome II and loss of heterozygosity for EXT-linked markers on chromosomes II and 8. *Am. J. Hum. Genet.* **56**, 1125-1131.

Huangfu, D. and Anderson, K. V. (2006). Signaling from Smo to Ci/Gli: conservation and divergence of hedgehog pathways from Drosophila to vertebrates. *Development* **133**, 3-14.

Huangfu, D., Liu, A., Rakeman, A. S., Murcia, N. S., Niswander, L. and Anderson, K. V. (2003). Hedgehog signaling in the mouse requires intraflagellar transport proteins. *Nature* **426**, 83-87.

Ingervall, B. and Thilander, B. (1972). The human spheno-occipital synchondrosis. I. The time of closure appraised macroscopically. *Acta Odontol. Scand.* **30**, 349-356.

Jeong, J. and McMahon, A. P. (2004). Growth and pattern of the mammalian neural tube are governed by partially overlapping feedback activities of the hedgehog antagonists patched 1 and Hhip1. *Development* **132**, 143-154.
Koyama, E., Leatherman, J. L., Noji, S. and Pacifici, M. (1996). Early chick limb cartilaginous elements possess polarizing activity and express *Hedgehog*-related morphogenetic factors. *Dev. Dyn.* **207**, 344-354.
Koziel, L., Kunath, M., Kelly, O. G. and Vortkamp, A. (2004). Ext1-dependent heparan sulfate regulates the range of Ihh signaling during endochondral ossification. *Dev. Cell* **6**, 801-813.
Kreiborg, S., Marsh, J. L., Cohen, M. M., Liversage, M., Pedersen, H., Skovby, F., Borgesen, S. E. and Vannier, M. W. (1993). Comparative three-dimensional analysis of CT-scans of the calvaria and cranial base in Apert and Crouzon syndromes. *J. Craniomaxillofac. Surg.* **21**, 181-188.
Lanske, B., Karaplis, A. C., Lee, K., Lutz, A., Vortkamp, A., Pirro, A., Karperien, M., Defize, L. H. K., Ho, C., Mulligan, R. et al. (1996). PTH/PTHrp receptor in early development and Indian hedgehog-regulated bone growth. *Science* **273**, 663-666.
Lin, F., Hiesberger, T., Cordes, K., Sinclair, A. M., Goldstein, L. S. B., Somlo, S. and Igarashi, P. (2003). Kidney-specific inactivation of the KIF3A subunit of kinesin-II inhibits renal ciliogenesis and produces polycystic kidney disease. *Proc. Natl. Acad. Sci. USA* **100**, 5286-5291.
Maeda, Y., Nakamura, E., Nguyen, M.-T., Suva, L. J., Swain, F. L., Razzaque, M. S., Mackem, S. and Lanske, B. (2007). Indian hedgehog (Ihh) produced by postnatal chondrocytes is essential for maintaining a growth plate and trabecular bone. *Proc. Natl. Acad. Sci. USA* **104**, 6382-6387.
Mak, K. K., Chen, M.-H., Day, T. F., Chuang, P.-T. and Yang, Y. (2006). Wnt/β-catenin signaling interacts differentially with Ihh signaling in controlling endochondral bone and synovial joint formation. *Development* **133**, 3695-3707.
Marszalek, J. R., Ruiz-Lozano, P., Roberts, E., Chen, K. R. and Goldstein, L. S. (1999). Situs inversus and embryonic ciliary morphogenesis defects in mouse mutants lacking the KIF3A subunit of kinesin-II. *Proc. Natl. Acad. Sci. USA* **96**, 5043-5048.
May, S. R., Ashique, A. M., Karlen, M., Wang, B., Shen, Y., Zarbalis, K., Reiter, J. F., Ericson, J. and Peterson, A. S. (2005). Loss of retrograde motor for IFT disrupts localization of Smo to cilia and prevents the expression of both activator and repressor functions of Gli. *Dev. Biol.* **287**, 378-389.
McMahon, A. P., Ingham, P. W. and Tabin, C. J. (2003). Developmental roles and clinical significance of hedgehog signaling. *Curr. Top. Dev. Biol.* **53**, 1-114.
Murcia, N. S., Richards, W. G., Yoder, B. K., Mucenski, M. L., Dunlap, J. R. and Woychik, R. P. (2000). The Oak Ridge Polycyctic Kidney (orpk) disease gene is required for left-right axis determination. *Development* **127**, 2347-2355.
Nakamura, E., Nguyen, M.-T. and Mackem, S. (2006). Kinetics of tamoxifen-regulated Cre activity in mice using a cartilage-specific CreER^{T} to assay temporal activity windows along the proximodistal limb skeleton. *Dev. Dyn.* **235**, 2603-2612.
Nakamura, T., Aikawa, T., Enomoto-Iwamoto, M., Iwamoto, M., Higuchi, Y., Pacifici, M., Kinto, N., Yamaguchi, A., Noji, S., Kurisu, K. et al. (1997). Induction of osteogenic differentiation by hedgehog proteins. *Biochem. Biophys. Res. Commun.* **237**, 465-469.
Namimatsu, S., Ghazizadeh, M. and Sugisaki, Y. (2005). Reversing the effects of formalin fixation with citraconic anhydride and heat: a universal antigen retrieval method. *J. Histochem. Cytochem.* **53**, 3-11.
Olsen, B. R., Kolpakova, E., McBratney-Owen, B., Li, X., Zhou, J. and Fukai, N. (2005). Genetic and epigenetic determinants of skeletal morphogenesis – role of cellular polarity and ciliary function in skeletal development and growth. *Oral Biosci. Med.* **213**, 57-65.
Ovdhinnikov, D. A., Deng, J. M., Ogunrinu, G. and Behringer, R. R. (2000). Col2a1-directed expression of Cre recombinase in differentiating chondrocytes in transgenic mice. *Genesis* **26**, 145-146.
Pacifici, M., Shimo, T., Gentili, C., Kirsch, T., Freeman, T. A., Enomoto-Iwamoto, M., Iwamoto, M. and Koyama, E. (2005). Syndecan-3: a cell surface heparan sulfate proteoglycan important for chondrocyte proliferation and function during limb skeletogenesis. *J. Bone Miner. Metab.* **23**, 191-199.
Park, T. J., Haigo, S. L. and Wallingford, J. B. (2006). Ciliogenesis defects in embryos lacking inturned or fuzzy function are associated with failure of planar cell polarity and hedgehog signaling. *Nat. Genet.* **38**, 303-311.
Pazour, G. J., Dickert, B. L., Vucica, Y., Seeley, E. S., Rosenbaum, J. L., Witman, G. B. and Cole, D. G. (2000). Chlamydomonas IFT88 and its mouse homologue polycystic kidney disease gene tg737, are required for assembly of cilia and flagella. *J. Cell Biol.* **151**, 709-718.
Roberts, G. J. and Blackwood, H. J. (1983). Growth of the cartilages of the mid-line cranial base; a radiographic and histological study. *J. Anat.* **136**, 307-320.
Rosenbaum, J. L. and Witman, G. B. (2002). Intraflagellar transport. *Nat. Rev. Mol. Cell Biol.* **3**, 813-825.
Scherft, J. P. and Daems, W. T. (1967). Single cilia in chondrocytes. *J. Ultrastruc. Res.* **19**, 546-555.
Shimazu, A., Nah, H.-D., Kirsch, T., Koyama, E., Leatherman, J. L., Golden, E. B., Kosher, R. A. and Pacifici, M. (1996). Syndecan-3 and the control of chondrocyte proliferation during endochondral ossification. *Exp. Cell Res.* **229**, 126-136.
Shimo, T., Gentili, C., Iwamoto, M., Wu, C., Koyama, E. and Pacifici, M. (2004). Indian hedgehog and syndecan-3 coregulate chondrocyte proliferation and function during chick limb skeletogenesis. *Dev. Dyn.* **229**, 607-617.
Singla, V. and Reiter, J. F. (2006). The primary cilium as the cell's antenna: signaling at a sensory organelle. *Science* **313**, 629-633.
Sorokin, S. P. (1968). Reconstructions of centriole formation and ciliogenesis in mammalian lungs. *J. Cell Sci.* **207**, 207-230.
St-Jacques, B., Hammerschmidt, M. and McMahon, A. P. (1999). Indian hedgehog signaling regulates proliferation and differentiation of chondrocytes and is essential for bone formation. *Genes Dev.* **13**, 2076-2086.
Stickens, D., Zak, B. M., Rougier, N., Esko, J. D. and Werb, Z. (2005). Mice deficient in Ext2 lack heparan sulfate and develop exostoses. *Development* **132**, 5055-5068.
Tamamura, Y., Otani, T., Kanatani, N., Koyama, E., Kitagaki, J., Komori, T., Yamada, Y., Costantini, F., Wasisaka, S., Pacifici, M. et al. (2005). Developmental regulation of Wnt/β-catenin signals is required for growth plate assembly, cartilage integrity, and endochondral ossification. *J. Biol. Chem.* **280**, 19185-19195.
The, I., Bellaiche, Y. and Perrimon, N. (1999). Hedgehog movement is regulated through tout-velu-dependent synthesis of a heparan sulfate proteoglycan. *Mol. Cell* **4**, 633-639.
Vortkamp, A., Lee, K., Lanske, B., Segre, G. V., Kronenberg, H. M. and Tabin, C. J. (1996). Regulation of rate of cartilage differentiation by Indian hedgehog and PTH-related protein. *Science* **273**, 613-622.
Xiao, Z., Zhang, S., Mahlios, J., Zhou, G., Mangenhelmer, B. S., Guo, D., Dallas, S. L., Maser, R., Calvet, J. P., Bonewald, L. et al. (2006). Cilia-like structures and polycystin-1 in osteoblasts/osteocytes and associated abnormalities in skeletogenesis and Runx2 expression. *J. Biol. Chem.* **281**, 30884-30895.
Yin, M., Gentili, C., Koyama, E., Zasloff, M. and Pacifici, M. (2002). Antiangiogenic treatment delays chondrocyte maturation and bone formation during limb skeletogenesis. *J. Bone Miner. Res.* **17**, 56-65.
Young, B., Minugh-Purvis, N., Shimo, T., St-Jacques, B., Iwamoto, M., Enomoto-Iwamoto, M., Koyama, E. and Pacifici, M. (2006). Indian and sonic hedgehog regulate synchondrosis growth plate and cranial base development and function. *Dev. Biol.* **299**, 272-282.
Zelzer, E., McLean, W., Ng, Y. S., Fukai, N., Reginato, A. M., Lovejoy, S., D'Amore, P. A. and Olsen, B. R. (2002). Skeletal defects in VEGF(120/120) mice reveal multiple roles of VEGF in skeletogenesis. *Development* **129**, 1893-1904.
Zhang, Q., Murcia, N. S., Chittenden, L. R., Richards, W. G., Michaud, E. J., Woychik, R. P. and Yoder, B. K. (2003). Loss of Tg737 protein results in skeletal patterning defects. *Dev. Dyn.* **227**, 78-90.